International Journal of Materials Engineering 2016, 6(3): 77-84
DOI: 10.5923/j.ijme.20160603.03

Evaluation of Ultrasonic Attenuation in Mortars Structures Using the Argand Diagram

Hassan Bita*, Bouazza Faiz, Ali Moudden, Hicham Lotfi, El Houssaine Ouacha, Mustapha Boutaib

Laboratory of Metrology and Information Processing, Ibn Zohr University, Faculty of Sciences, Agadir, Morocco

Abstract The work presents a new method that tracks the total attenuation of the ultrasonic waves in a mortar during hydration. The method is based on a representation in the complex plane of reflection coefficient of waves backscattered by the mortar layer which takes the form of a circle in the vicinity of a resonance. Monitoring the diameter of the circle during all stages of hydration shows its sensitivity to changes in the microstructure of the material. A strong correlation exists between the diameter of the Argand circle and attenuation on samples with different compositions and at different temperatures. The correlation shows the ability of the parameter to detect the physical and chemical changes in the material and its accuracy for differentiating the phases of hydration.

Keywords Attenuation, Ultrasonic, Mortar, Reflexion coefficient, Argand Diagram

1. Introduction

Ultrasound is widely used in many fields of science. Their applications are generally classified into two categories: high power ultrasound that can change the environment in which they propagate as in the case of sonochemistry [1-3] and very low power ultrasound used in diagnosis, measurement and non-destructive control. Recently the ultrasonic application is also extended to the civil engineering field. Several research studies have been conducted to characterize, in a nondestructive way, the cementitious materials [4-7]. These techniques have proven to estimate the mechanical and structural properties of these materials by measuring the velocity and attenuation.

The ultrasonic wave propagation and interaction of these waves with the material are widely used for non-destructive evaluation. The properties of the propagation of these waves are directly related to the mechanical and structural properties of the materials in which propagate. In non-homogeneous or non-elastic media, the interaction of the wave with the microstructure causes attenuation losses. These losses are due to a combination of absorption and diffusion. The effect of absorption losses is due to the viscoelastic behavior of materials and scattering losses are due to the heterogeneity of the material [8-11]. Much research has shown that the attenuation is a function of frequency, others have shown that it also depends on the grain diameter of material [9-13].

* Corresponding author:
hassan.bita51@gmail.com (Hassan Bita)
Published online at http://journal.sapub.org/ijme

Cementitious materials are sometimes multiphase and are characterized by the existence of heterogeneity of different natures and also their evolution over time because of the very long process of hydration of mixed products. In these products, the nature misunderstood of the ultrasonic wave propagation greatly complicates the task of quantifying contributions of the various mechanisms to the total attenuation. Therefore, there are no models that explain accurately mitigation mechanisms in these materials [8, 11]. In this work, we present a new method to follow and evaluate the ultrasonic attenuation in a mortar during all phases of hydration using the Argand diagram.

The resonant scattering theory [14, 15] provides that the propagation of sound waves in the material generates resonances in its thickness wherein each resonance is characterized by its frequency and its width. We are interested in resonances of the reflection coefficient of a plane mortar structure. In the vicinity of an isolated resonance representation in the complex plane of its imaginary part as a function of its real part (Argand Diagram) is a circle [16]. During its evolution mortar transforms from a viscous state to viscoelastic solid state then to elastic state. This transformation is accompanied by a variation of the ultrasonic attenuation. We show the sensitivity of the diameter of the circle Argand to the variation of the ultrasonic attenuation in the cementitious material during hydration. Correlations established experimentally possible to estimate the damping of ultrasound in the mortar only via the measurement of the diameter of the circle. This dimensionless diameter is later named parameter D.

2. Materials and Methods

2.1. Experimental Device

The experimental device described in detail in a previous work [17], consists of a parallel sided container enclosing a thick layer of mortar d_m= 15mm, irradiated at normal incidence by an ultrasonic wave emitted by a transducer of central frequency 0,5MHz which acts as emitter and receiver. The recording of the signals reflected by the Plexiglas / mortar / glass structure, is 15min all three days.

2.2. Theory

Assuming that the three layers structures plexiglas, mortar and glass are flat, and by placing in the context of the theory of linear systems, the signal reflected by the mortar layer can be written as a sum of echo reflected by the interface Plexiglas / mortar and all the echoes that have undergone multiple reflections within the cementitious material:

$$S_{rm}(t) = S_{r2}(t) + S_{r3}(t) + S_{r3'}(t) + \ldots \quad (1)$$

Signal processing in the frequency plan allows to write:

$$S_{r\,m}(f) = S_0(f)[R_{\underline{p}\,m} + T_{\underline{p}\,m} R_{\underline{m}\,g} T_{\underline{m}\,p} \exp(-j(2k_m d_m)\times \sum_{n=0}^{\infty}(R_{\underline{m}\,g} R_{\underline{m}\,p} \exp(-j2k_m d_m))^n] \quad (2)$$

With:

$S_0(f)$: The Fourier transform of the signal emitted by the transducer passing through the coupling medium (water + Plexiglas) twice (round trip).

$R_{i/j} = \frac{Z_j - Z_i}{Z_j + Z_i}$: The reflection coefficient of the i/ j interface.

$T_{i/j} = \frac{2Z_i}{Z_j + Z_i}$: The transmittance of the i/j interface.

z_i : The acoustic impedance of the medium i and the letters p, m, and g represent the Plexiglas, mortar and glass.

k_m: The wave vector and d_m the thickness of the mortar.

The reflexion coefficient of the mortar layer can be written as a series of Debye:

$$R = \frac{S_{rm}(t)}{S_0(f)} = R_{\underline{p}\,m} + T_{\underline{p}\,m} R_{\underline{m}\,g} T_{\underline{m}\,p} \exp(-j(2k_m d_m)\times \sum_{n=0}^{\infty}(R_{\underline{m}\,g} R_{\underline{m}\,p} \exp(-j2k_m d_m))^n \quad (3)$$

Experimentally terms of order n ≥1 in equation (1) are not visible (Figure 1), in this case the complex reflection coefficient of the mortar is then:

$$R = R_{\underline{p}\,m} + T_{\underline{p}\,m} R_{\underline{m}\,g} T_{\underline{m}\,p} \exp(-j(2k_m d_m) \quad (4)$$

The mortar is a mitigating environment and attenuation of the ultrasonic wave α_m expressed in the imaginary part of the wave vector k_m as follows:

$$k_m = \frac{2\pi f}{v_m} - j\,\alpha_m \quad (5)$$

Where: v_m : The speed of the wave in the mortar.

In the vicinity of a resonance, the Argand diagram is a circle with center $\Omega\,(R_{\underline{p}\,m}, 0)$ and diameter D :

$$D = 2\,T_{\underline{p}\,m} R_{\underline{m}\,g} T_{\underline{m}\,p} \exp(-2\,\alpha_m\,d_m) = 2\,(1 - R^2_{\underline{p}\,m})\,R_{\underline{m}\,g} \exp(-2\,\alpha_m\,d_m) \quad (6)$$

2.3. Measures

The experimental reflexion coefficient of mortar layer s obtained using the Fourier transforms ratio of the two echoes $Sr_2(t)$ and $Sr_3(t)$ reflected by the two mortar interfaces:

$$R = R_{\underline{p}\,m} \times \frac{S_{r2}(f) + S_{r3}(f)}{S_{r2}(f)} \quad (7)$$

To measure the total attenuation of the ultrasonic waves, we use the spectra ratio method of these two echoes as it is detailed in [17].

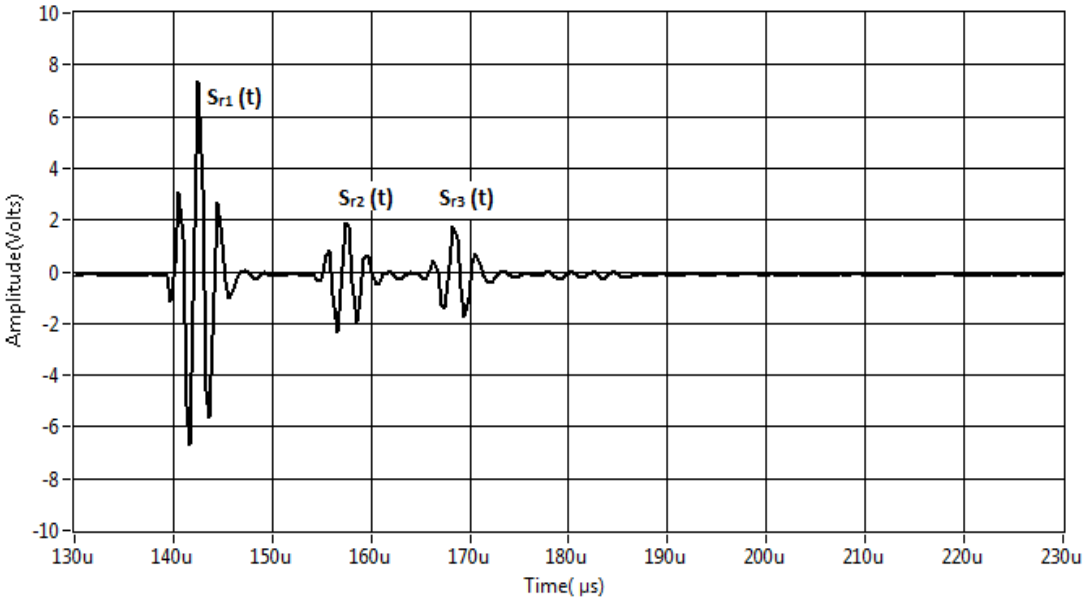

Figure 1. Example of signal reflected by the various interfaces of the Plexiglas / mortar / glass structure

$$\alpha_m = -\frac{1}{2d_m}\ln\left(\frac{T_{\frac{p}{m}}\,R_{\frac{m}{g}}\,T_{\frac{m}{p}}}{R_{\frac{p}{m}}}\frac{|S_{r3}(f)|}{|S_{r2}(f)|}\right) \quad (8)$$

The calculation of the Fourier transforms and the application of different signal processing techniques is performed using the LabView environment as a platform.

3. Results and Discussion

3.1. Variation of Parameter D with Frequency

A representation of the experimental reflection coefficient modulus as a function of frequency for a mortar made of sand grain with size d = 315 µm at room temperature T = 25 ℃ is carried on the figure 2. The representation shows the resonance frequencies of the mortar structure corresponding to the minimum of the reflection coefficient. Equation (4) shows that the resonance frequencies where the minima of the reflection coefficient lie are such that:

$$f_0 = (2n+1)\frac{v_m}{4d_m} \quad (9)$$

With n is the order of apparition of a minimum.

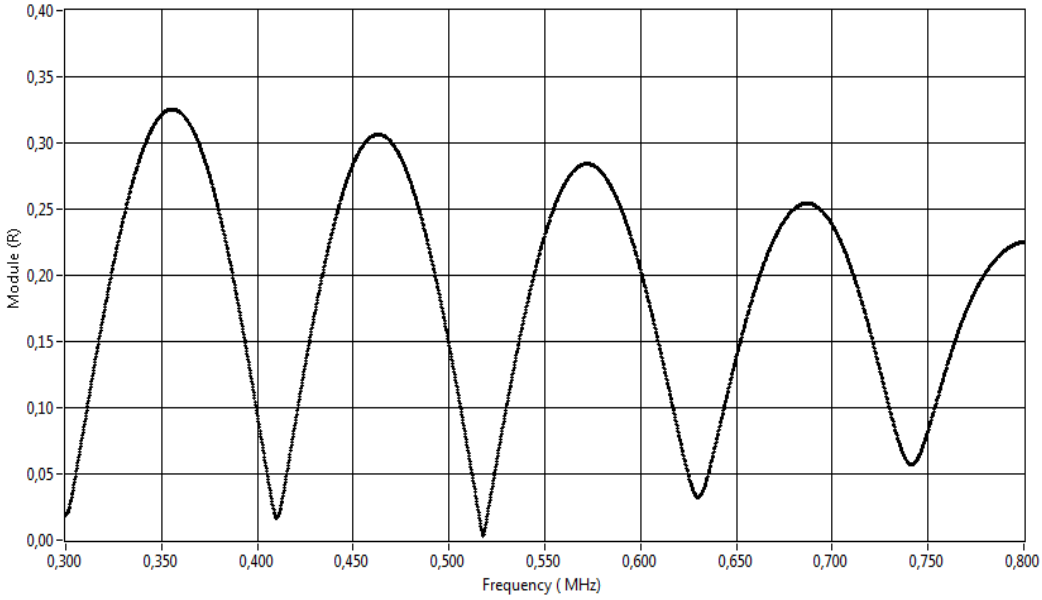

Figure 2. A representation of the reflection coefficient modulus as a function of the frequency

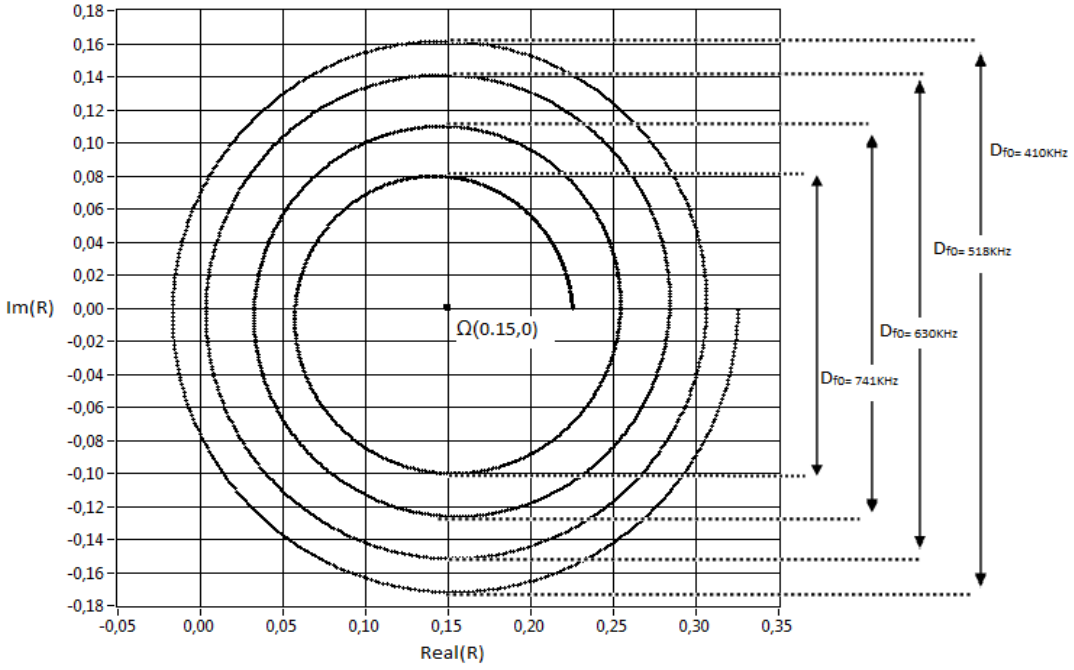

Figure 3. Variation of the diameter of the Argand circle with frequency

In Figure 3, we presented in the complex plane the reflection coefficient. This representation shows that each resonance is characterized by a circle of diameter D which decreases with frequency. The propagation of sound waves in the material leads to attenuation losses that are related to the viscosity, thermal conductivity and the physico-chemical changes in the propagation medium structure. Several studies show that the attenuation increases with frequency [9-11, 18]. Thus the decrease in the amplitude of the modulus of the reflection coefficient and the diameter of the Argand circle with frequency can be explained by an increase of the ultrasound attenuation in the mortar.

3.2. Sensitivity of the Parameter D to the Evolution of the Mortar Microstructure

Monitoring the variation of the parameter D, corresponding to the resonance of order n = 5 during the evolution of the mortar from a young age to curing for 70 hours, is used to trace the curves representing the diameter D and its derivative function over time in Figure 4. in the figure we can distinguish five stages and four characteristic points. The four points corresponding to the extrema of the function derivative $\frac{dD}{dt} = f(t)$, used to locate the time in each of the mortar hydration phases described previously [17]. During the first stage called initial phase, which lasts about one hour, the mixed products are completely separate in water [19, 20] the diameter D remains constant D≅12. The end of the first step and the start of the second are marked by the first feature point A_1. In this step, we observe a linear decrease of the parameter D over time; the derivative function is almost constant at this stage. In this phase, it begins the formation of first hydration products, but the bonds between the particles of cement are not yet well established; the material remains plastic and workable. The curves shown in Figure 5 show that during this time the total attenuation increases progressively in the opposite direction to the variation of the parameter D. From the characteristic point A_2 we observe a rapid decrease of parameter D accompanied by a sharp increase in attenuation, and from the time t = 5h measuring the diameter of the circle is not possible because the signal is completely attenuated in the mortar [17]. At this stage, significant changes in the structure of the material appear, the rate of formation of hydrated products is very large and bonds between constituting of the mortar become solid. This step corresponds to the beginning of the intake phase, which is considered the most important in the structure of cementitious products. Taking phase is divided into two stages: the first is the acceleration period characterized by significant and continuous reduction of the diameter D and the second is the period of deceleration whose beginning is marked in the figure by the partial characteristic point A_3 where the parameter D starts to increase. In fact, the curve representing the derivative function is decreasing indicating a decrease in the formation rate of the hydration products. The end of the setting period is marked by the characteristic point A_4 from which the variation of the parameter D is very low indicating the start of the final stage of the hydration of the mortar. The diameter D tends to stabilize on a long-term time interval.

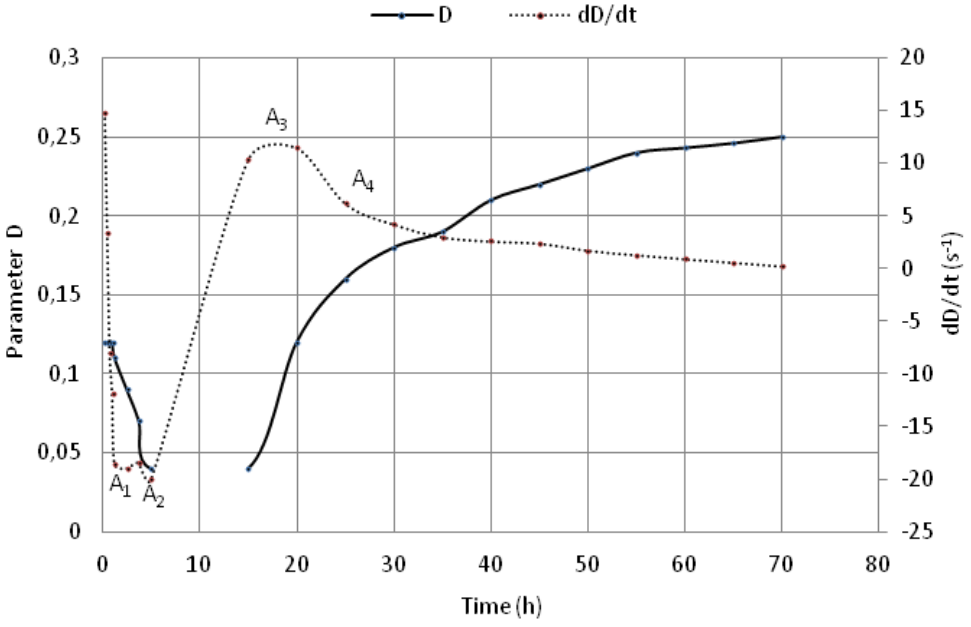

Figure 4. Representation of parameter D and its derivative dD/dt according to the time

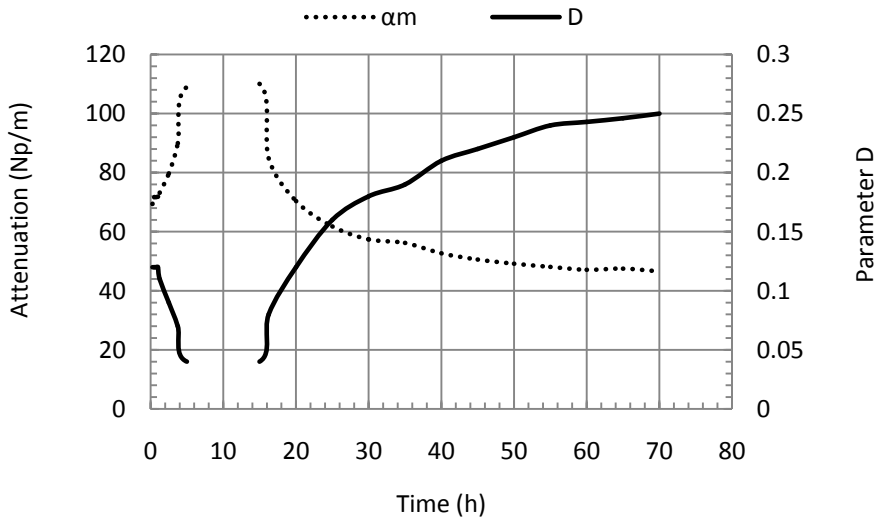

Figure 5. Variation of parameter D and attenuation according to time

3.3. Correlation between the Parameter D and the Attenuation

The accuracy of the parameter D in the detection of different periods of hydration of the mortar, shows its sensitivity to any variation or change in the material microstructure. Figure 5 shows the variation of the parameter D compared to the attenuation in the mortar over time. We find that the attenuation is going through the same phases of hydration as parameter D. In the early hours, when the attenuation begins to increase, we observe a strong decrease of the parameter D. At the end of the setting period and during the hardening phase, the behavior of the two parameters is reversed; we note a decrease in attenuation over time against an increase in the diameter of the Argand circle. In the last phase, the rate of change of these two parameters becomes low. These important observations therefore show that there is a strong correlation between the two studied parameters.

In Table 1, we gathered the curves representing the evolution of the parameter D depending on the total attenuation α_m in two main phases of the mortar, liquid and solid for four mortars solutions prepared with sand grains of different sizes or different temperatures. The results show an exponential decrease of the parameter D when the total attenuation increases, this applies to all the prepared solutions in all mortar hydration phases. The results also show that the relationship between the parameter D and the total attenuation is unique and follows the law:

$$D = D_0\, e^{-L\gamma} \tag{10}$$

Where D_0 is the diameter of Argand circle at zero attenuation, it is dimensionless and L is the distance traveled by the wave in the material in meters.

These results are in good agreement with our theoretical predictions (equation 6). Table 2 compares the derived parameters of the exponential regression. Important observations can be captioned. Indeed, the high values of the correlation coefficients which are close to 1, indicates a strong correlation between the parameter D and the total attenuation and demonstrate the sensitivity and the dependence of this parameter to the variation of the attenuation regardless of the particle size sand, temperature and any other unknown mortar curing time. The empirical law (10) expressing the relationship between the parameter D and the total attenuation provides constant values of parameter D_0 that represents the diameter of the Argand circle at zero attenuation. The regression results show that the parameter D_0 is more important in the solid phase than in the liquid one for all mortar solutions. Table 2 shows the highest values of D_0 in the solid phase for solutions prepared with diameter of sand grains of d=500µm, 315µm and at temperature T = 42℃ compared to other solutions. Indeed the measured values of D_0 are approximate because this parameter depends on the reflection coefficients of the two mortar interfaces (Equation 5) and can vary due to the change of the acoustic impedance of the mortar during hydration. Similarly the route of the ultrasonic wave in the mortar is subject to variations during the transition of the mortar from the liquid phase to the solid one. This variation may be due to a change in the thickness of the mortar. Indeed, we notice a decrease of the thickness of the material structure in the first hours of hydration, a decrease which is particularly important that the diameter of sand is large and the temperature is high. The mortar thickness reduction can be attributed to a chemical removal, which is not good for the material and can cause microscopic cracks which can seriously degrade the performance of long-term material [21-23]. However, we can not confirm this in the present work until the study is not extended at different W / C ratio; several studies have shown the influence of W / C ratio and hardening temperature on the removal of chemicals of cement pastes at an early age [21, 23]. We also note the absence of this phenomenon in the mortar prepared at room temperature.

Table 1. Exponential fit of the parameter D depending of the total attenuation

	[0,25h -- 5h]	[15h -- 70h]
d=250 µm (T=42 ℃)	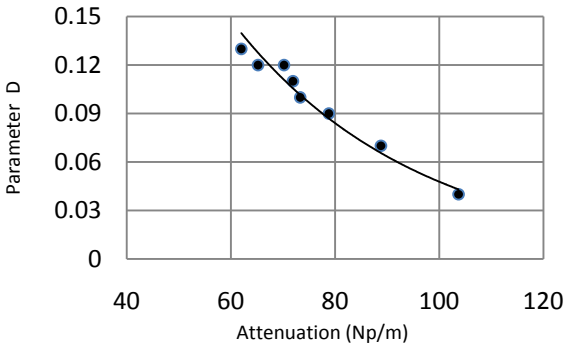	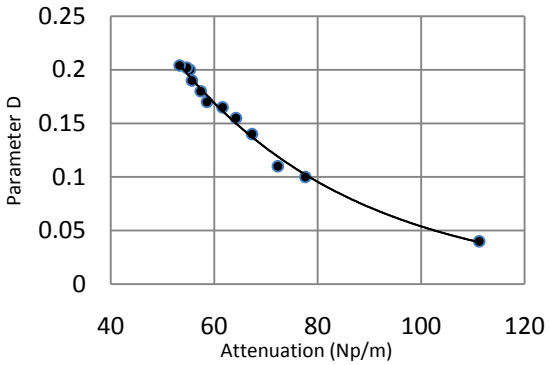
d=315 µm (T=42 ℃)	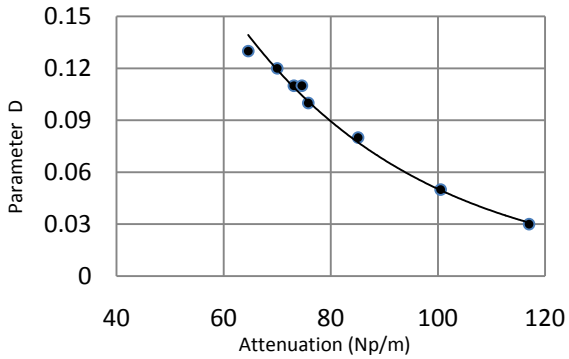	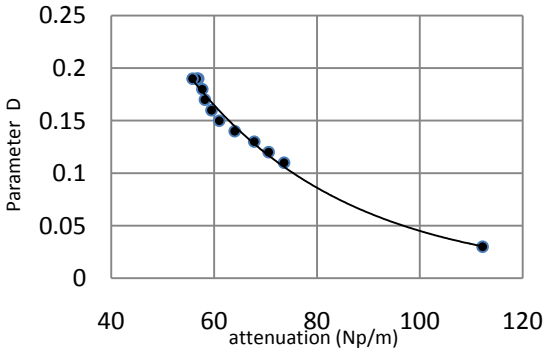
d=500 µm (T=42 ℃)	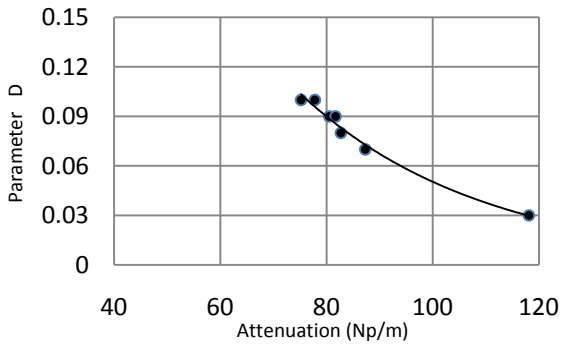	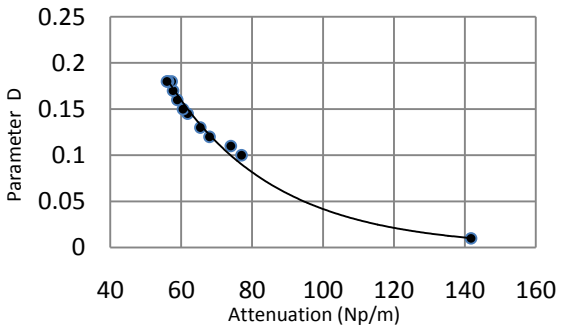
d=315 µm (T=25 ℃)	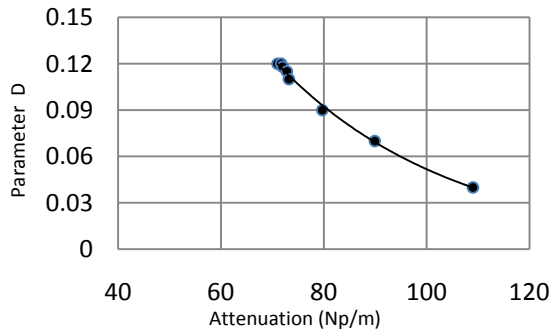	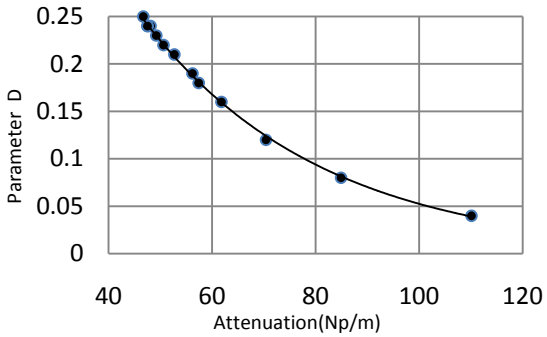

Table 2. Parameters of the exponential regression

Parameters of the regression	T=42 ℃						T=25 ℃	
	d=250 µm		*d=315 µm*		*d=500 µm*		*d= 315 µm*	
	[0,25h--5h]	[15h--70h]	[0,25h--5h]	[15h--70h]	[0,25h--5h]	[15h--70h]	[0,25h--5h]	[15h--70h]
D_0	0,804	0,941	0,800	1,153	0,914	1,191	0,938	0,959
L	0,028	0,029	0,028	0,032	0,029	0,033	0,029	0,029
R^2	0,97	0,99	0,98	0,99	0,99	0,99	0,99	0,99

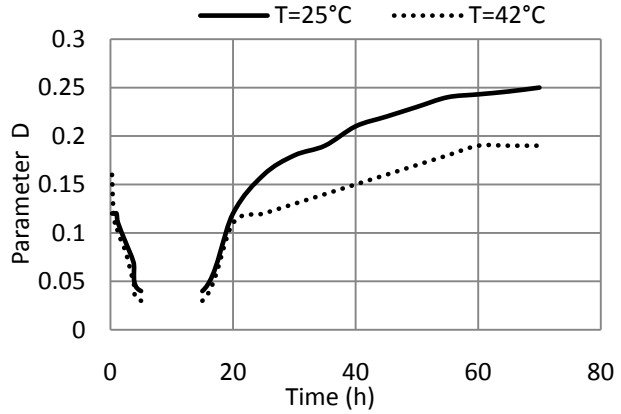

Figure 6. Temperature effect on the evolution of the parameter D

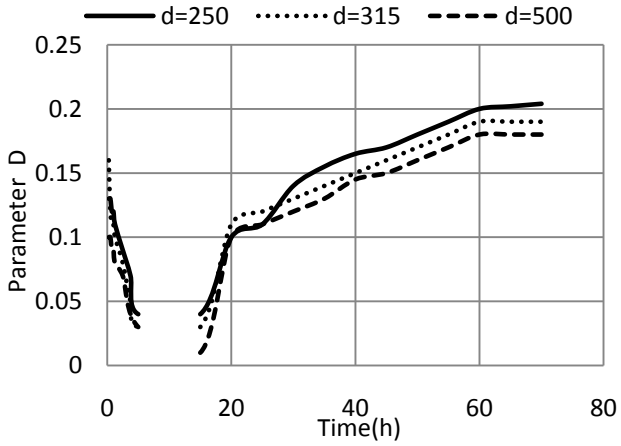

Figure 7. Effect of the size of sand grains on the evolution of the parameter D

The effect of the temperature and the particle size of the sand on the evolution of the parameter D according to the mortar of the hydration time is shown in the figures 6 and 7. The influence of the sand grain size is clearly observed on the diameter of the Argand circle. It is particularly important that the diameter of the sand grains is low .This can only be explained by an increase of the attenuation which can be due to an increase in porosity. Several studies have shown that the mechanical properties of cement-based materials decrease with porosity [24-27]. Further work showed that the compressive strength increases as the size of sand grains decreases [28, 29]. Similarly, the impact of temperature on the change of the parameter D is remarkable in the hardening phase. Figure 6 shows that the cured mortar at temperature T=42 ℃ has a lowest parameter D compared to hardened at ambient temperature so high ultrasonic attenuation. This shows that temperature has a major role in the development of mechanical mortar properties. Low hardening temperatures result in a uniform distribution of hydrates, while higher temperatures lead to a coarser pore structure [30].

4. Conclusions

This work presents a non-destructive characterization method of cementitious materials based on the representation of Argand. The extracted representation of this parameter is the diameter of the circle Argand. The ability of the parameter to detect the different physical and chemical transformations of the material is not affected by the variation of the temperature or the type of sand. Our experimental measurements on mortar samples show that the D parameter is especially important as temperature is low and the diameter of the sand grains is great. We also showed that the diameter of the Argand circle follows an exponential distribution of the total attenuation of ultrasound in the mortar. The fact that neither the general shape of the curves or correlation is affected by temperature and the nature of the sand, shows that the parameter D may be used as an indicator of the total attenuation; its measurement can therefore inform us on the microstructure and the health status of the material at all times. Parameter D can be used also to measure with great precision the thickness of the mortar.

REFERENCES

[1] Suslick, K. S. Sonochemistry. science, 247(4949), 1439-1445 (1990).

[2] Kumar, B., Smita, K., Kumar, B., & Cumbal, L. Ultrasound promoted and SiO_2/CCl_3COOH mediated synthesis of 2-aryl-1-arylmethyl-1H-benzimidazole derivatives in aqueous media: An eco-friendly approach. Journal of Chemical Sciences, 126(6), 1831-1840 (2014).

[3] Kumar, B., Smita, K., Cumbal, L., & Debut, A. Ficus carica (Fig) Fruit Mediated Green Synthesis of Silver Nanoparticles and its Antioxidant Activity: a Comparison of Thermal and Ultrasonication Approach. BioNanoScience, 1-7 (2016).

[4] Chekroun, M., Le Marrec, L., Abraham, O., Durand, O., & Villain, G. Analysis of coherent surface wave dispersion and attenuation for non-destructive testing of concrete. Ultrasonics, 49(8), 743-751 (2009).

[5] Soltani, F., Goueygou, M., Lafhaj, Z., & Piwakowski, B. Relationship between ultrasonic Rayleigh wave propagation and capillary porosity in cement paste with variable water content. NDT & E International, 54, 75-83 (2013).

[6] Thomas. Voigt, Zhihui .Sun, Surendra. P. Shah. Comparison of ultrasonic wave reflection method and maturity method in evaluating early-age compressive strength of mortar, Cement & Concrete Composites, 28 pp 307–316 (2006).

[7] Soltani,F., Lafhaj, Z., Goueygou, M. Experimental determination of the relationship between porosity and surface wave parameters of fully and partially saturated cement paste. International Symposium on Non Destructive Testing in Civil Engineering, Nantes, France, 30 June -3 rd July, pp 851-856 (2009).

[8] L.J. Jacobs, J.O. Owino. Effect of aggregate size on attenuation of Rayleigh surface waves in cement-based materials. J. Eng. Mech. 126(11): 1124–1130 (2000).

[9] E.P. Papadakis. Revised grain-scattering formulas and tables. J. Acous. Soc. Am. 37(4): 703– 710 (1965).

[10] Saniie. J, Wang .T, Bilgutay .N. M. Analysis of homomorphic processing for ultrasonic grain characterization. IEE transaction on ultrasonics, ferroelectrics and frequency control. 34(3): 365-375 (1989).

[11] Aggelis .D, Polyzos .D, Philippidis.T. Wave dispersion and attenuation in fresh mortar: theoretical predictions vs. experimental results. J Mech. Phys. Solids. 53: 857–883 (2005).

[12] Evans. A. G, Tittmann. B. R, Ahlberg. L, Khuri-Yakub. B. T, Kino. G. S. Ultrasonic attenuation in ceramics. J. Appl. Phys. 49. 2669–2679 (1978).

[13] Saniie. J, Bilguty. N. M. Quantitative grain size evaluation using ultrasonic backscattered echoes. J. Acoust. Soc. Am. 80. 175– 184 (1986).

[14] R. Fiorito, W. Madigosky, H. Überall. Resonance theory of acoustic waves interacting with an elastic plate. J. Acoust. Soc. Am. 66, 1857 (1979).

[15] R. Fiorito, W. Madigosky, H. Überall. Theory of ultrasonic resonances in a viscoelastic layer. J. Acoust. Soc. Am. 77, 489 (1985).

[16] S. Derible, P. Rembert, J.L. Izbicki. Experimental Determination of Acoustic Resonance Width via the Argand Diagram, Acta Acustica 84 270–279 (1998).

[17] Hassan Bita, Ali Moudden, Bouazza Faiz, Hicham Lotfi. Non Destructive Characterization of Mortars by the Frequency Offset Method. Journal of Civil Engineering Research, Vol. 5 No. 6, pp. 136-143 (2015).

[18] Aggelis. D.G, Philippidis. T. P.. Ultrasonic wave dispersion and attenuation in fresh mortar. NDT&E International 37: 617–631 (2004).

[19] G. Ye, Experimental study and numerical simulation of the development of microstructure and permeability of cementitious materials, PhD Thesis, Delft university of technology, Delft (2003).

[20] Gregor. Trtnik, Matija. Gams, Recent advances of ultrasonic testing of cement based materials at early ages, Ultrasonics 54: 66–75 (2014).

[21] Mounanga P, Khelidj A, Loukili A, Baroghel-Bouny V. Predicting $Ca(OH)_2$ content and chemical shrinkage of hydrating cement pastes using analytical approach. Cem Concr Res; 34(2):255–65 (2004).

[22] M. Bouasker, P. Mounanga, P. Turcry, A. Loukili, A. Khelidj. Chemical shrinkage of cement pastes and mortars at very early age: Effect of limestone filler and granular inclusions. Cement & Concrete Composites 30, pp 13–22 (2008).

[23] Erika Holt. Contribution of mixture design to chemical and autogenous shrinkage of concrete at early ages. Cement and Concrete Research 35 464– 472 (2005).

[24] Zoubeir Lafhaj, Marc Goueygou, Assia Djerbi, Mariusz Kaczmarek. Correlation between porosity, permeability and ultrasonic parameters of mortar with variable water / cement ratio and water content. Cement and Concrete Research 36 625 – 633(2006).

[25] M.G. Hernàndez, J.J. Anaya, L.G. Ullate, M. Cegarra, T. Sanchez. Application of a micromechanical model of three phases to estimating the porosity of mortar by ultrasound. Cement and Concrete Research 36 617–624(2006).

[26] S. Maalej, Z. Lafhaj, M. Bouassida. Micromechanical modelling of dry and saturated cement paste: Porosity assessment using ultrasonic waves. Mechanics Research Communications 51 8– 14(2013).

[27] Xudong Chen, Shengxing Wu, Jikai Zhou. Influence of porosity on compressive and tensile strength of cement mortar. Construction and Building Materials 40 869–874 (2013).

[28] Seok Hee Kang, Tae-Ho Ahn, Dong Joo Kim. Effect of grain size on the mechanical properties and crack formation of HPFRCC containing deformed steel fibers. Cement and Concrete Research 42 710–720(2012).

[29] R. Sugrañez, J.I. Álvarez, M. Cruz-Yusta, I. Mármol, J. Morales, L. Sánchez. Controlling microstructure in cement based mortars by adjusting the particle size distribution of the raw materials. Construction and Building Materials 41 139–145 (2013).

[30] Knut O. Kjellsen, Rachel J. Detwiler, Odd E. Gjørv. Development of microstructures in plain cement pastes hydrated at different temperatures. Cement and Concrete Research. 21 179189 (1991).